first component q_1 offers a means to measure the instability of X_e:

$$q_1 = q_1(X_e) \tag{11}$$

A station-keeping maneuver Δv is introduced at X_e by canceling the q_1 component out. Taking the design of 2-axis x-y controller as an example, the Δv is represented as $(\delta v_x, \delta v_y)$, and the q_1 component after the maneuver is

$$q_1 = q_1\left((x_e, y_e, z_e, vx_e + \delta v_x, vy_e + \delta v_y, vz_e)\right) \tag{12}$$

Setting q_1 to 0,we get a relationship that satisfied by $\delta v_x, \delta v_y$:

$$q_1\left((x_e, y_e, z_e, vx_e + \delta v_x, vy_e + \delta v_y, vz_e)\right) = 0 \tag{13}$$

Then the optimal Δv can be computed numerically by a general constrained optimization procedure.

5. NUMERICAL SIMULATION AND ANALYSIS

5.1 Station-keeping of Lissajous trajectory

In the following simulation, a Lissajous trajectory of earth-moon L_1 point is chosen as the reference trajectory. The initial state in CRTBP synodic coordinates is X_0(0.829, -0.000393, -0.0476, 0.00279, 0.1077, -0.04066). The maximum amplitudes in x, y, z direction are A_x=8253km, A_y=25140km, A_z=18335km respectively.

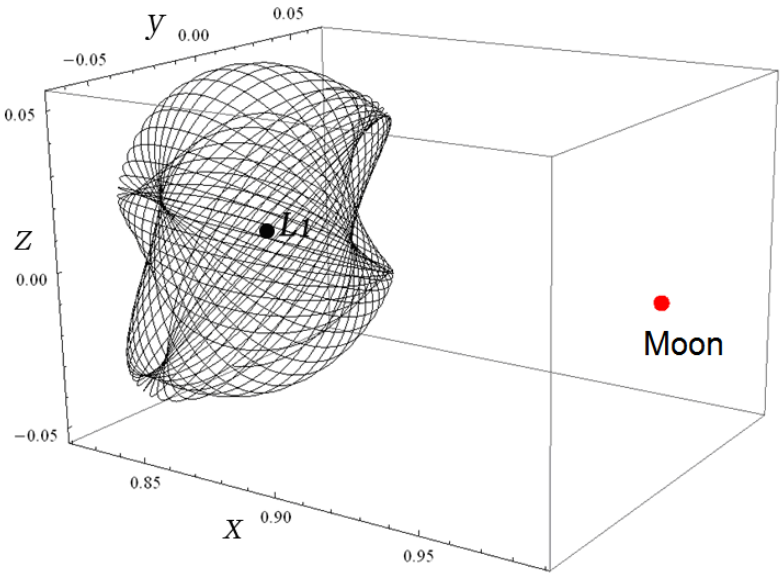

Fig.1 The reference Lissajous trajectory used in the simulation

Without station-keeping maneuver, the q_1 unstable component tends to increase exponentially, which can be clearly seen in Table 1.

Table. 1 Orbital states expressed in center manifold coordinates

t	q_1	p_1	q_2	p_2	q_3	p_3
0	0.0000337963	0.000052645	0.0000193309	0.456657	0.477664	0.178919
0.5	0.000976189	0.000103956	0.403984	0.239483	0.413708	0.283534
1	0.00350324	0.000166302	0.356949	0.23886	0.0750113	0.478553
1.5	0.0171132	0.000254882	0.132355	0.419008	0.44577	0.0802302
2	0.0730465	0.000158375	0.487655	0.00682569	0.233545	0.384257
2.5	0.27692	0.0000315699	0.236857	0.431862	0.25347	0.378311
3	0.997551	0.0161548	0.26608	0.404465	0.482882	0.00316409

Assuming a maneuver $(\delta v_x, \delta v_y)$ is introduced at $t=2$, the orbital states before the maneuver is：

$$X_{t=2} = (0.841653, -0.0497382, 0.0241285, -0.0498749, -0.00818304, -0.085897)$$

Using the inversed coordinate transformation (computed up to order 6), we get q_1

$$\begin{aligned} q_1(\delta v_x, \delta v_y) = & -74.795\delta v_x^5\delta v_y + 114.138\delta v_x^4\delta v_y^2 + 23.427\delta v_x^4\delta v_y - \\ & 242.38\delta v_x^3\delta v_y^3 - 5.19259\delta v_x^3\delta v_y^2 - 2.946\delta v_x^3\delta v_y - 331.452\delta v_x^2\delta v_y^4 + \\ & 134.717\delta v_x^2\delta v_y^3 - 20.906\delta v_x^2\delta v_y^2 + 10.998\delta v_x^2\delta v_y - 184.57\delta v_x\delta v_y^5 + \\ & 126.663\delta v_x\delta v_y^4 - 35.496\delta v_x\delta v_y^3 + 12.307\delta v_x\delta v_y^2 - 2.7184\delta v_x\delta v_y - \\ & 12.1934\delta v_x^6 + 19.197\delta v_x^5 - 3.9524\delta v_x^4 + 0.9902\delta v_x^3 - 4.5667\delta v_x^2 + \\ & 2.93986\delta v_x - 7.31865\delta v_y^6 + 22.0542\delta v_y^5 - 10.504\delta v_y^4 + 5.61\delta v_y^3 - \\ & 2.95318\delta v_y^2 + 1.73047\delta v_y - 0.0730465 \end{aligned} \tag{14}$$

Setting q_1 to 0, we get a implicit curve satisfied by δv_x and δv_y.

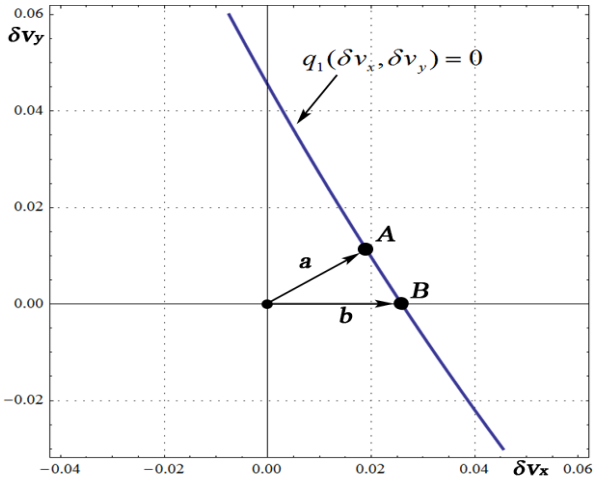

Fig .2 Implicit curve defined by $q_1(\delta v_x, \delta v_y) = 0$

In order to obtain the minimum $(\delta v_x, \delta v_y)$ value satisfying constraint $q_1(\delta v_x, \delta v_y) = 0$, a general numerical constrained optimization procedure is used. The result is:

$$\delta v_x = 19.5351 m/s, \delta v_y = 11.5619 m/s, \left|(\delta v_x, \delta v_y)\right| = 22.7 m/s$$

Assuming the time interval between consecutive station-keeping maneuver is fixed to 1 non-dimensional time unit (corresponding to 4.34913 days), all of the station-keeping maneuver can be computed accordingly. Setting the total flight time to $T = 10$, Table 2 sums up the Δv consumption for the 1 to 3 axes controller.

Table. 2 Station-keeping Δv (m/s) profiles for 3 kinds of controllers using the center manifold projection method

Maneuver sequence	**1**	**2**	**3**	**4**	**5**	**6**	**7**	**8**	**9**	**10**	$\sum \Delta v_i$
x axis controller	1.447	0.925	1.214	1.139	1.093	0.476	2.539	2.587	0.307	0.412	12.14
x-y axes controller	1.314	0.785	1.141	0.948	0.972	0.452	1.998	2.449	0.311	0.366	10.73
x-y-z controller	1.288	0.779	1.131	0.930	0.957	0.446	1.949	2.407	0.305	0.357	10.55

Figure 3 shows the q_1 curve of the x-y axes controller, indicating that the unstable component is indeed being cancelled out by the center manifold projection method.

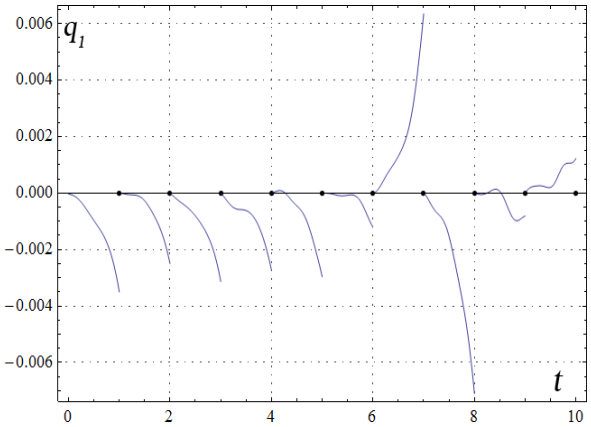

Fig. 3 q_1 curve of the simulation process using x-y axes controller

5.2 Comparison with Floquet mode approach

As the proposed station-keeping strategy doesn't rely on a specific orbit type to work, it's also suitable for the control of halo type orbits. In this case, we can compare its performance with the Floquet mode approach. The reference orbit is an earth-moon L_1 point halo orbit with x, y, z amplitudes $A_x = 10059km$ 、 $A_y = 26355km$ 、 $A_z = 16039km$ respectively.

Assuming the time interval between consecutive station-keeping maneuver is fixed to 7 days, the first 10 Δv s are calculated with different center manifold computation precision (higher computation order corresponding to higher precision). Table 3 sums up the Δv consumptions for these simulations.

It's evident that the Δv consumptions are closely related to the center manifold computation order. As the order increases, the center manifold computation becomes more precise, and the total Δv consumption decreases quickly. When the order of center manifold computation is larger than 13, the Δv consumption is significantly lower than the Floquet mode approach. In the case of order 15, the Δv consumption is about half of the Floquet mode approach.

Table. 3 Station-keeping Δv comparisons between Floquet mode approach and center manifold projection method

Maneuver sequence		**1**	**2**	**3**	**4**	**5**	**6**	**7**	**8**	**9**	**10**	$\sum \Delta v_i$
Floquet mode approach		1.752	0.175	0.109	0.206	0.325	0.117	0.168	0.069	0.213	0.265	3.403
center manifold projection method	Order 6	1.547	16.55	6.184	19.11	8.29	7.579	9.90	19.71	10.7	14.03	113.6
	Order 8	1.722	2.618	2.781	2.33	1.394	1.599	1.376	2.599	1.299	2.398	20.12
	Order 10	1.75	0.34	0.009	0.566	0.506	0.275	0.189	0.444	0.203	0.386	4.671
	Order 13	1.754	0.024	0.054	0.074	0.023	0.017	0.01	0.029	0.022	0.101	2.109
	Order 15	1.754	0.004	0.004	0.021	0.007	0.001	0.108	0.01	0.009	0.028	1.945

6. CONCLUSIONS

By taking advantage of the special dynamical structure of the collinear libration points, the definition of the libration point region is formulated; the transformation from synodic coordinates to the decoupled center manifold coordinates is derived. Based on this transformation, the error state can be projected to the nearest center manifold by introducing maneuver delta V. In this way, the unstable component can be canceled. The proposed station-keeping strategy fully integrates the dynamical property of collinear libration points, and is suitable for all kinds of libration point orbits. Finally, numerical simulations were performed on Lissajous orbit and halo orbit, verifying that this strategy can achieve good station-keeping performance.

Acknowledgements

This work was supported by the National Natural Science Foundation of China (Grant No. 11403013), the Fundamental Research Funds for the Central Universities (NO. 56XAA14093, 56YAH12036) and Postdoctoral Foundation of Jiangsu Province (NO.1301029B).

REFERENCES

Gómez, G., A. Jorba, J. Masdemont, and C. Simo (1991), Study refinement of semi-analytical halo orbit theory, Final Report, ESOC Contract No.:8625/89/D/MD(SC).

Gómez, G., Llibre, J., Martínez, R., and Simó, C. (2001), Dynamics and Mission Design Near Libration Points, Vol. I: Fundamentals: The Case of Collinear Libration Points, World Scientific Monograph Series, World Scientific Publishing Ltd., Singapore.

Gómez G, Mondelo J M (2001). The dynamics around the collinear equilibrium points of the RTBP[J]. Physica D: Nonlinear Phenomena, 157(4): 283-321.

Howell, K. C., Keeter, T.M. (1995), Station-Keeping Strategies for Libration Point Orbits: Target Point and Floquet Mode Approaches, Proceedings of the AAS/AIAA Spaceflight Mechanics Conference 1995, Advances in the Astronautical Sciences, Vol. 89, 1377-1396.

Howell K.C., Pernicka H.J. (1993), Station-Keeping Method for Libration Point Trajectories, Journal of Guidance, Control, and Dynamics, Vol. 16, No. 1, January-February, pp. 151-159.

Howell, K. C., S. C. Gordon (1994), Orbit determination error analysis and a station-keeping strategy for Sun-Earth L1 libration point orbits, The Journal of the Astronautical Sciences, 42, 207–228.

Jorba, A. and J. Masdemont (1999), Dynamics in the Center Manifold of the Collinear Points of the Restricted Three Body Problem, Physica D 132, 189–213.

Koon W S, Lo M W, Marsden J E, Ross S D (2007), Dynamical Systems, the Three-Body Problem and Space Mission Design[M]. Springer-Verlag New York Inc.

Y. Ren and J. Shan (2014), A Novel Algorithm for Generating Libration Point Orbits About the Collinear Points. Celestial Mechanics and Dynamical Astronomy, 120(1):57–75.